

Plasma Diagnostics: Spectroscopy

Onofrio Tudisco

Ricercatore ENEA

Lay-out

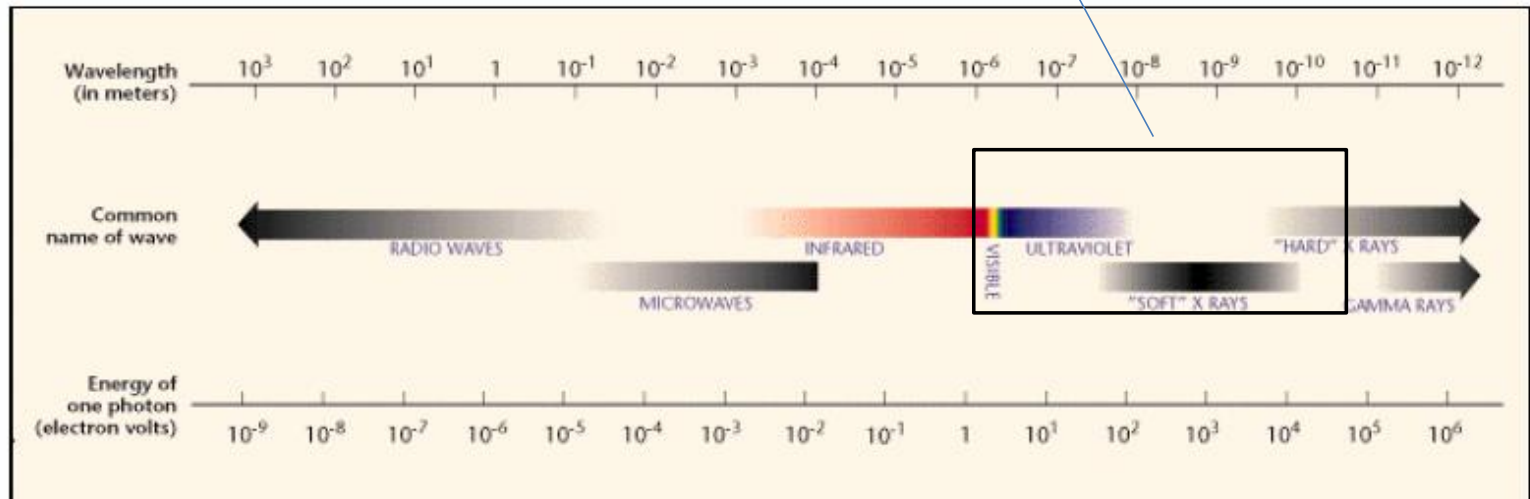
- Part I
 - Emission spectral range
 - Spectrometers
 - Line monitoring : D_α and particle balance
 - UV spectroscopy
 - X-ray spectroscopy
- Part II
 - bremsstrahlung
 - Active diagnostic : CXS
 - Active diagnostic : MSE
 - X ray tomography
 - Laser induced florescence

Tokamak spectroscopy

- For “spectroscopy” is intended those diagnostics that measure the line emission of partially ionized ions.
 - It can provide relevant information on
 - Amount of impurity present in the plasma
 - Plasma velocity
 - Plasma temperature
 - Other spectroscopy are used in plasma physics as :
 - Far infrared spectroscopy
 - RF spectroscopy
 - γ - spectroscopy
 - Neutron spectroscopy
- but are referred with different name.

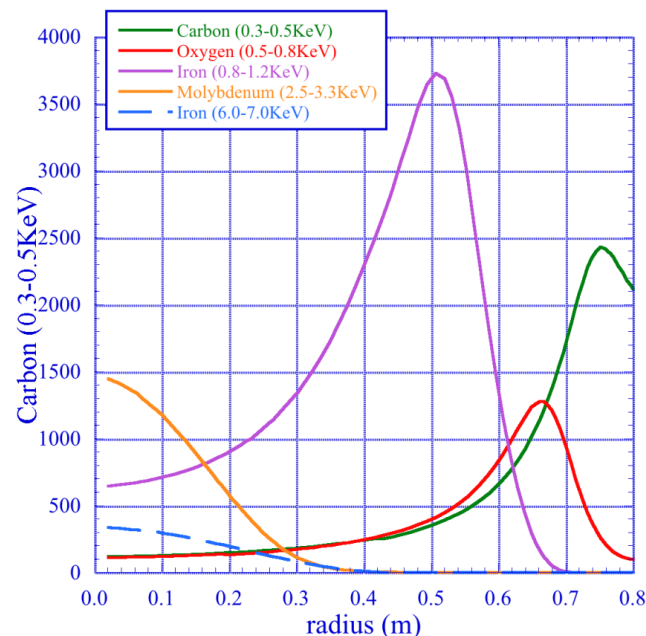
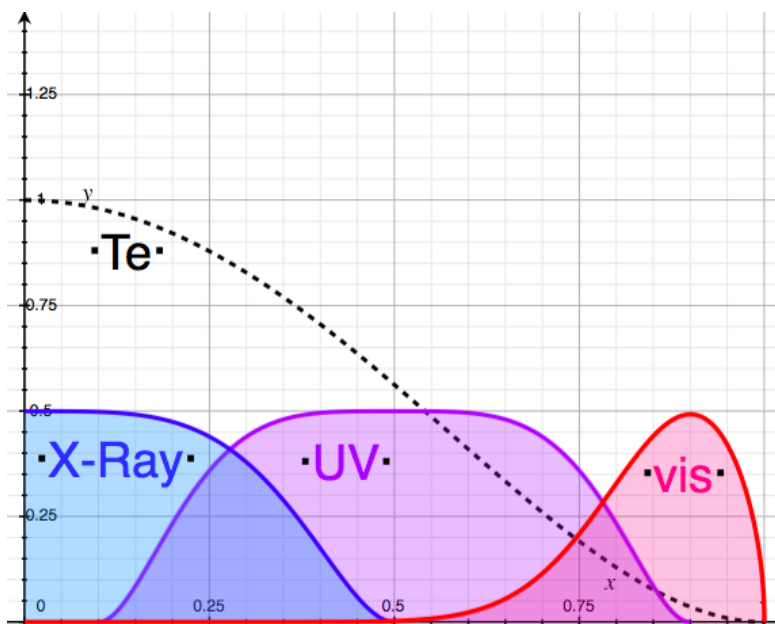
Spectral range

Impurity emission
range in tokamak



Radiation Regions

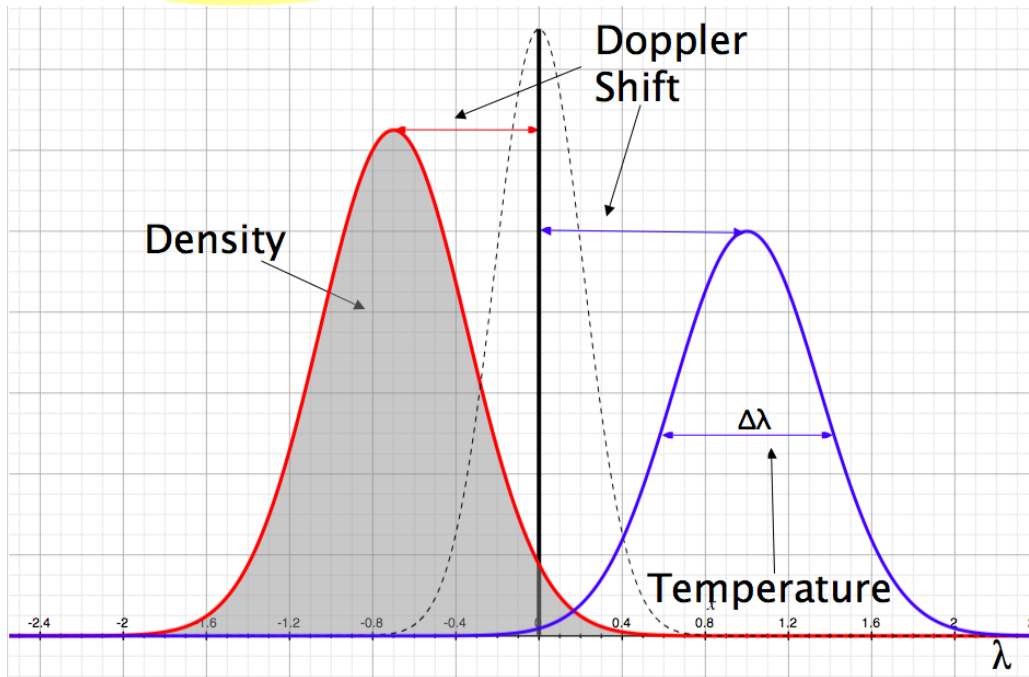
- T_e in tokamaks varies from few eV to keV
- Both line and continuum radiation are emitted over a large range of frequency
- Visible light is emitted at edge, UV at half radius, and soft X-ray in plasma core.



Information from spectral line

From line emission we can get :

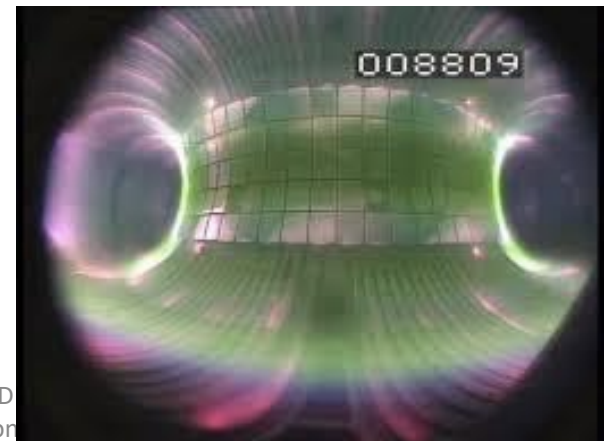
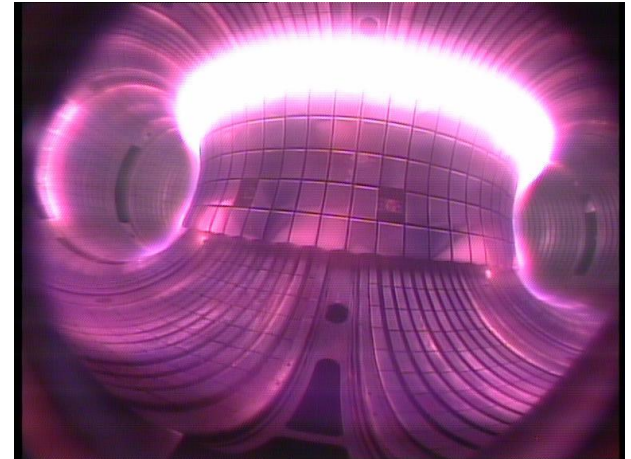
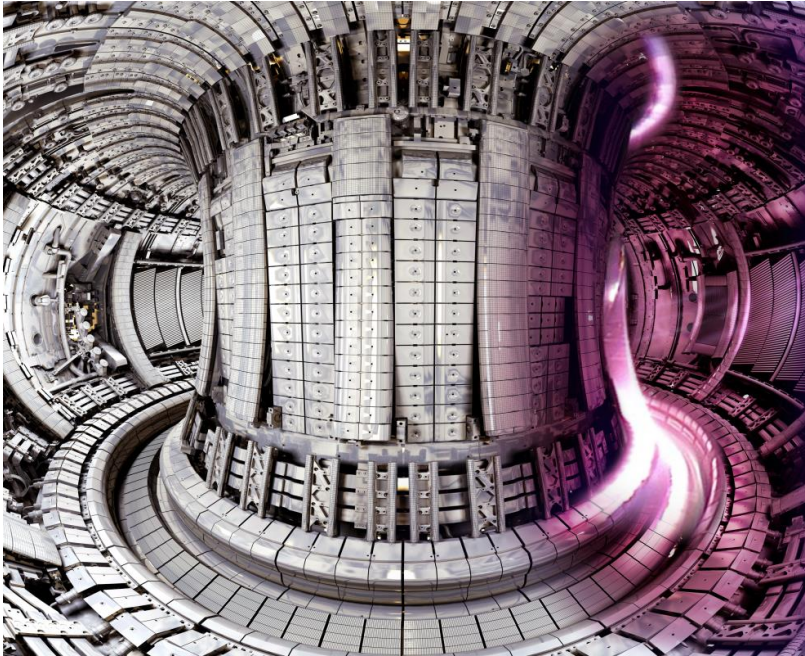
- Density of impurity (area below the line)
- Temperature (line width)
- Average velocity along the line sight (Doppler Shift)



Spectra measurements

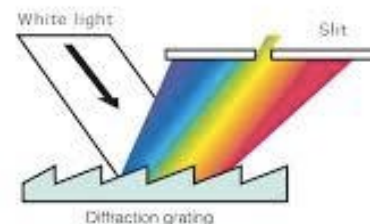
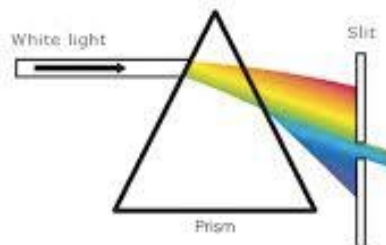
- Different kind of spectrometers are employed in plasma diagnostic: it depends on spectral range, resolution and measurements scope.
 - Grating spectrometer in visible range
 - Interferential filters (visible/NIR)
 - UV spectrometer
 - Soft X ray spectrometer

Plasma image in visible light

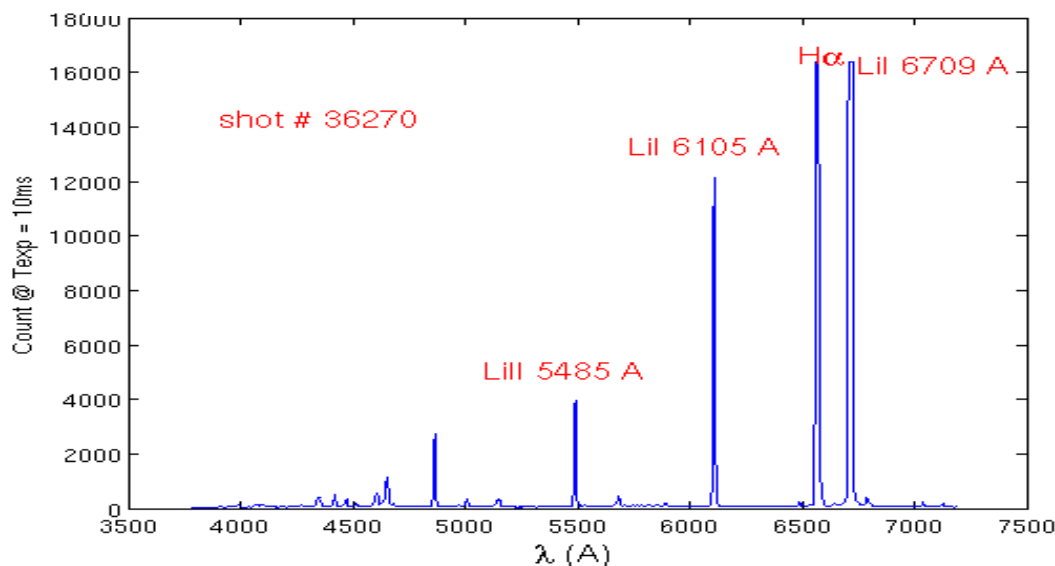


Example of spectrum in visible range

Sketch of
Spectrometer
layout

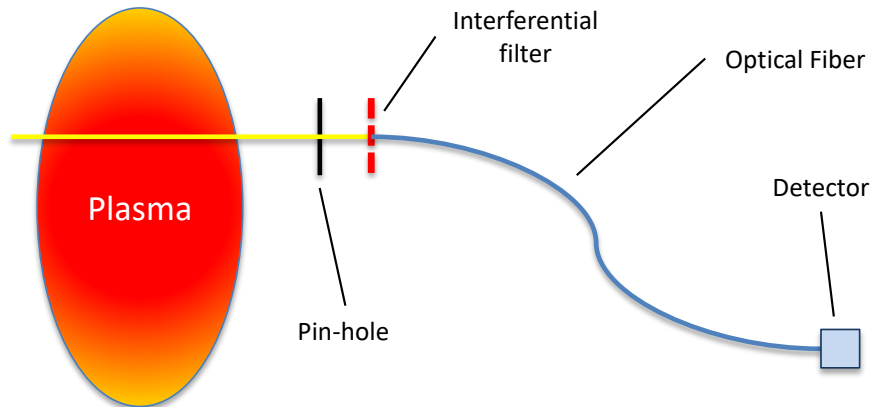


Visible
spectrum in
FTU



Line monitoring

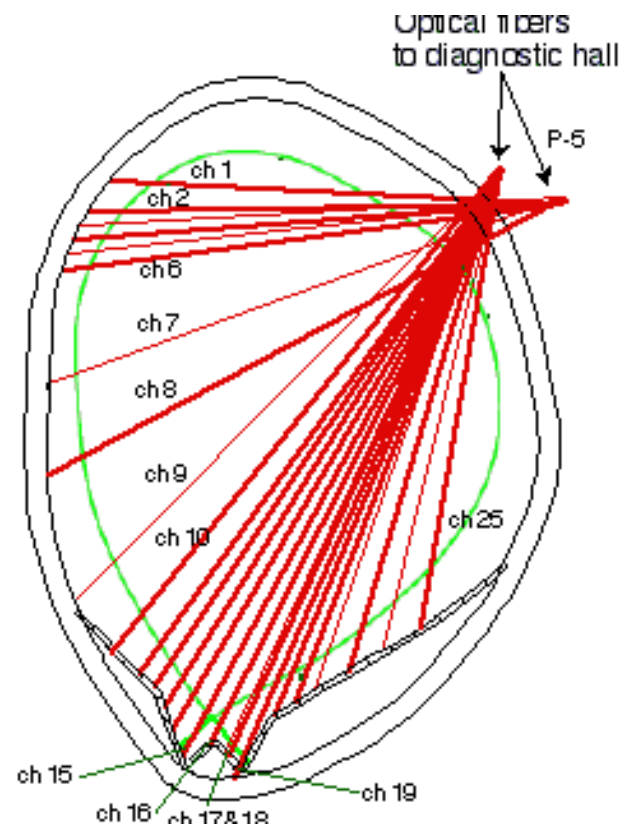
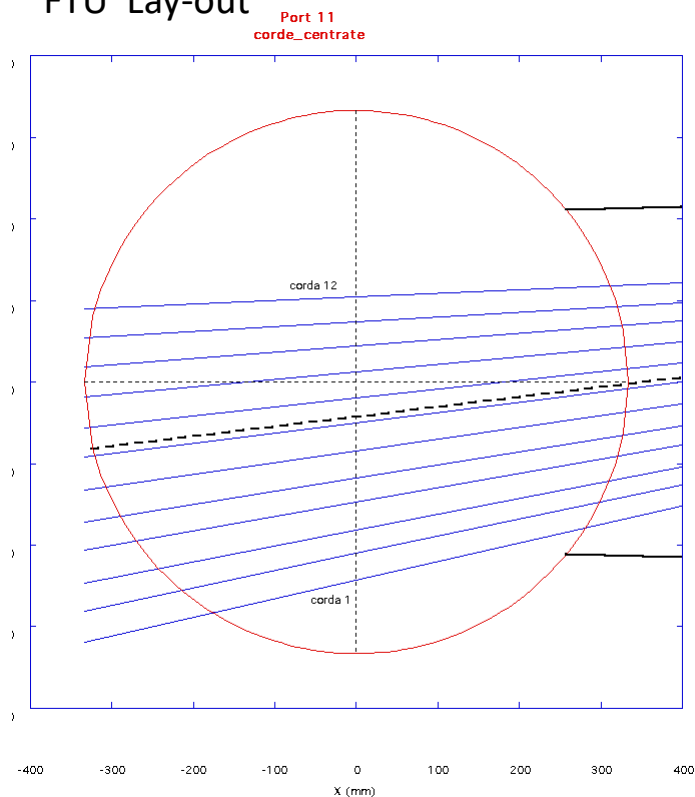
- Using interferential filters it is possible monitoring the evolution of a thin slice of spectrum.
 - examples: D_α , Li, bremsstrahlung,



D_α Diagnostic Layout

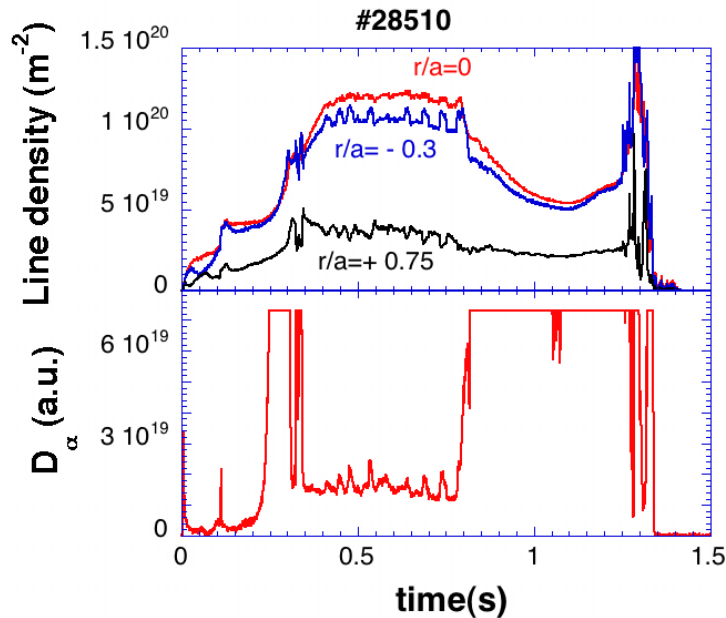
JT60 Lay-out

FTU Lay-out

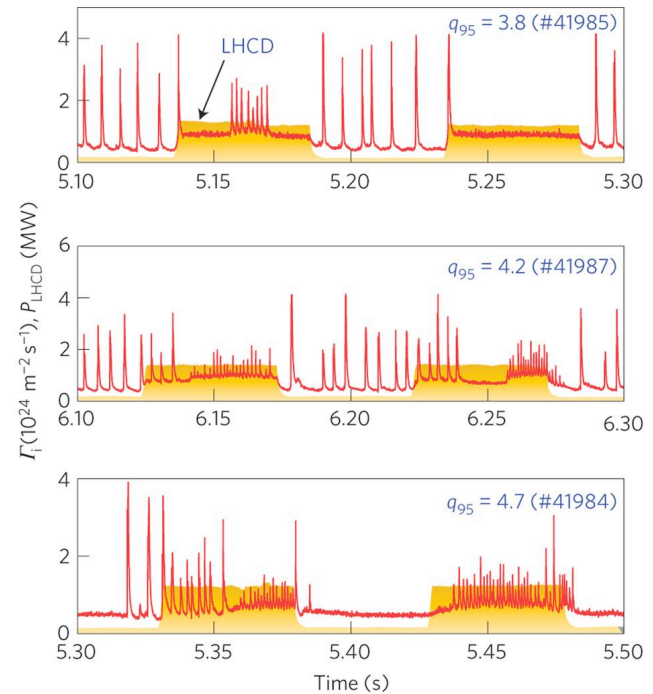


D_α monitor

D_α is used as a monitor for fast edge phenomena as MARFE and ELMS



D_α emission during MARFE in FTU



ELM control study at EAST tokamak

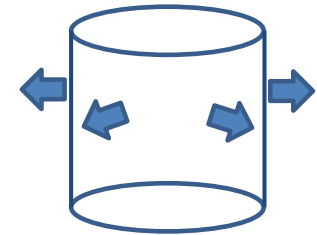
Particle Balance from D_α

From D_α it is possible to obtain the flux of neutral particle entering the plasma and the particle confinement time.

Consider a plasma cylinder of radius a . Ion balance eq., in steady state condition, is

$$\frac{1}{r} \frac{d}{dr} (r \Gamma_i) = n_o n_e S_o - n_i n_e \alpha$$

$$a \Gamma_i = \int_0^a n_o n_e S_o r dr$$



Neglecting recombination, and integrating over the plasma radius:
 D_α emission along a line is give by:

$$I_\alpha = \int_{-a}^a n_o n_e X B dr$$

neutral density is appreciable only at edge and S_o/XB is only weakly dependent on temperature and density

Γ : particle flux
 n_o : neutral particle density
 n_e : electron density
 n_i : ion density
 S_o : ionization rate
 α : recombination rate
 X : D_α excitation rate
 B : D_α branching ratio for de-excitation
 I_α : D_α mission

Particle Balance from D_α

we can rewrite the integral

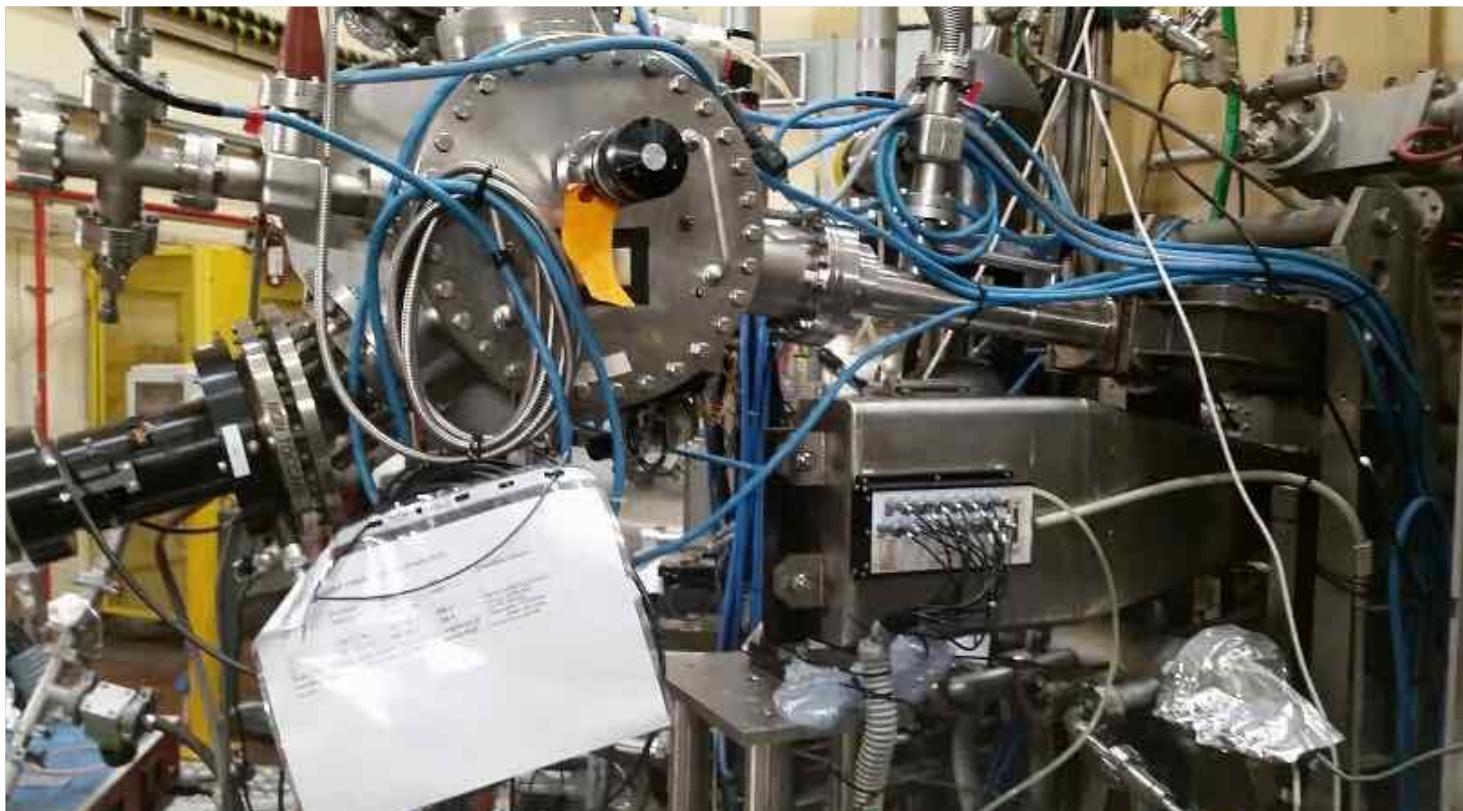
$$\int_0^a n_o n_e S_o r dr \cup a \frac{S_o}{XB} \int_0^a n_o n_e XB dr = \frac{1}{2} a \frac{S_o}{XB} I_\alpha$$

Hence the particle flux can be obtained as:

$$\Gamma_i = \frac{I}{a} \int_0^a n_o n_e S_o r dr \sim \frac{S_o}{XB} \int_0^a n_o n_e XB dr = \frac{I}{2} \frac{S_o}{XB} I_\alpha$$

Γ : particle flux
 n_o : neutral particle density
 n_e : electron density
 n_i : ion density
 S_o : ionization rate
 α : recombination rate
 X : $D\alpha$ excitation rate
 B : $D\alpha$ branching ratio for de-excitation

UV Spectrometer FTU



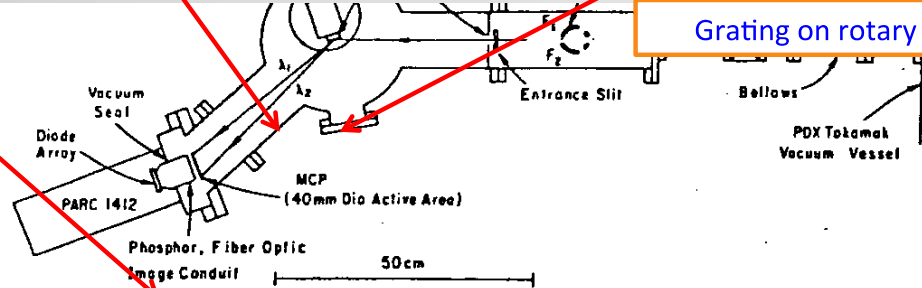
FTU UV spectrometer



Photodiode array



Grating on rotary table



rotary feedthrough. The grating positions are indexed by spring loading against a heavy pin, and the location of the spectrum is repeatable at the focal plane to within $\pm 20 \mu\text{m}$ on grating exchange (or 0.4 \AA with the 4000 \AA grating).

MCP

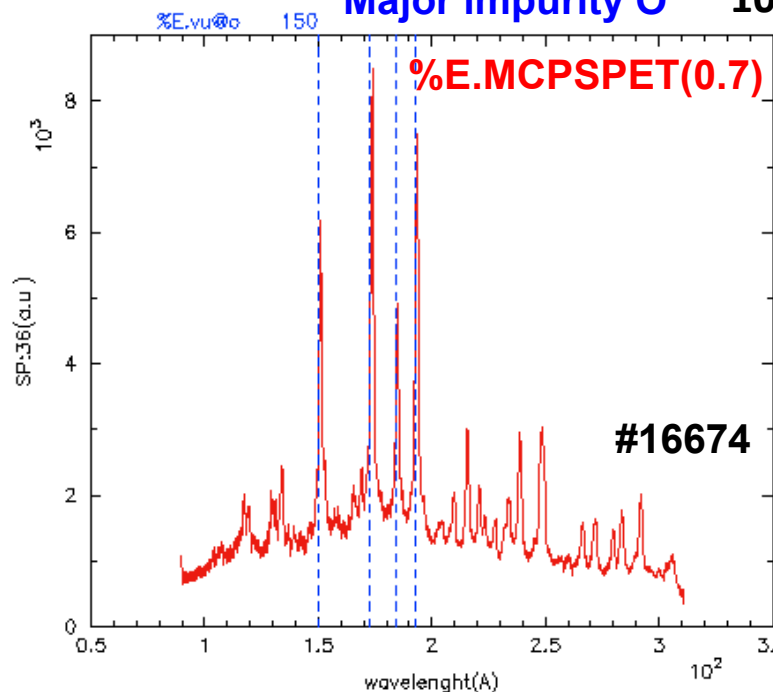


UV spectra

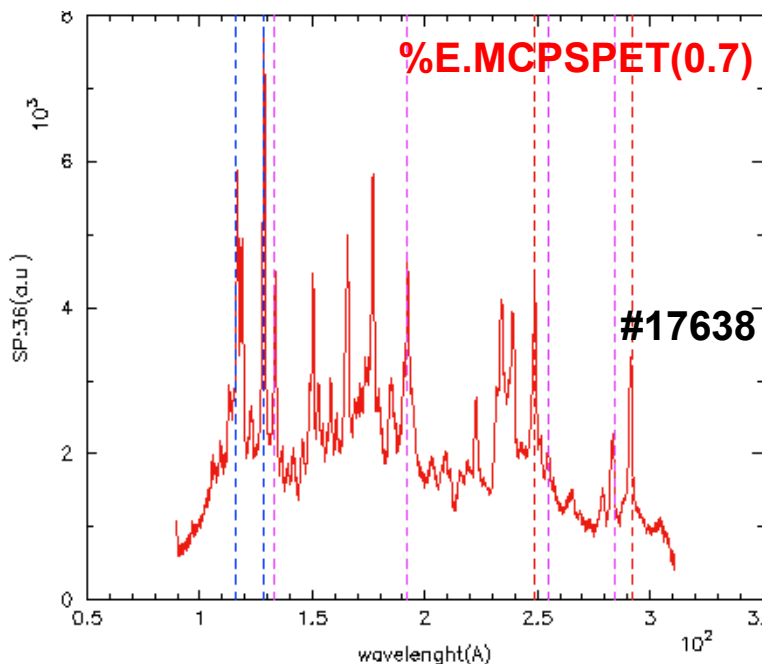
Major impurity O

100 – 300 Å

Metal impurity plasma

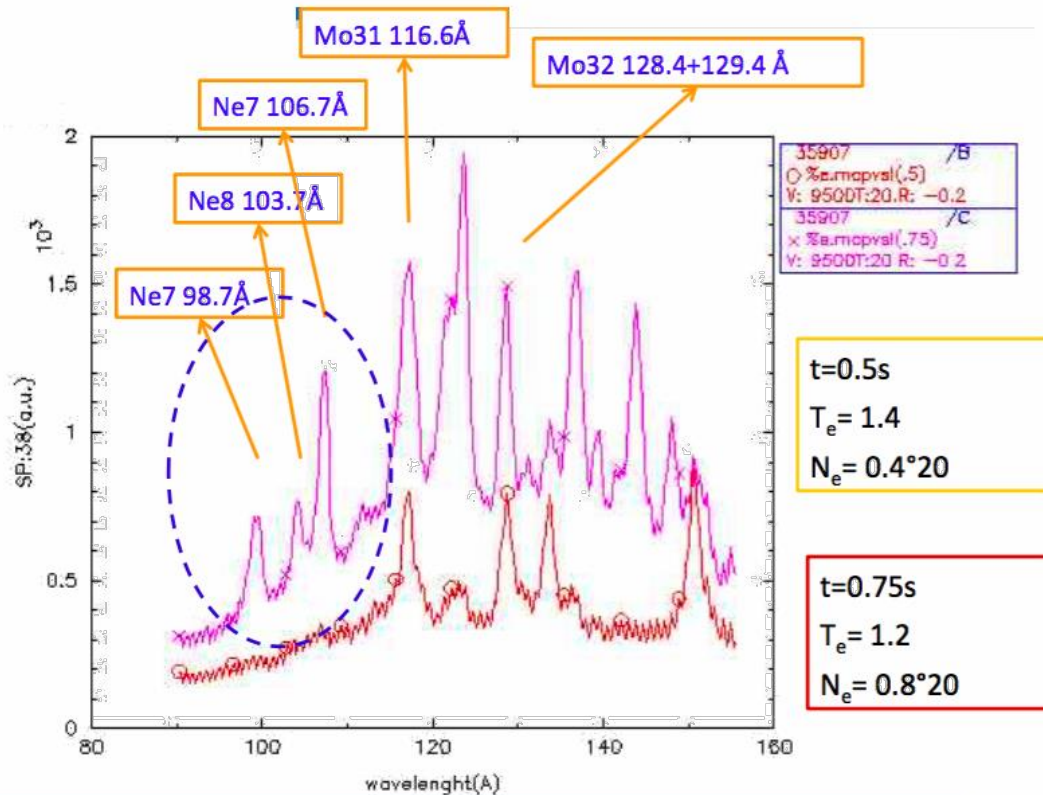


O VI ---> 150.08 Å
O VI ---> 173.084 Å
O VI ---> 184.05 Å



Mo XXXI ---> 116 Å
Mo XXXII ---> 128 Å
Ni XVII ---> 249 Å
Ni XVIII ---> 292 Å
Fe XXXIII ---> 133 Å

UV spectrum: Ne injection



Impurity transport

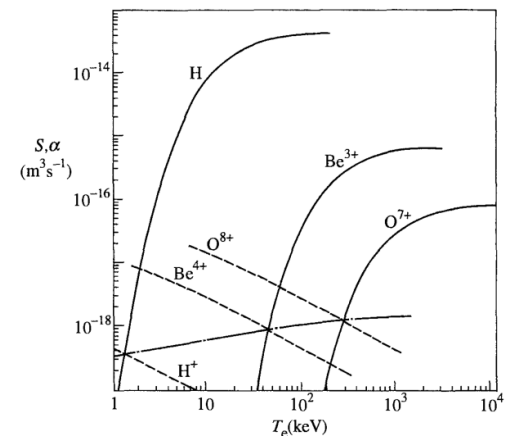
For each impurity species and ionization state we can write an equation for its diffusion in

$$\frac{fn_{z_j}}{ft} + \frac{1}{r} \frac{f}{fr} (r\Gamma_{z_j}) = -n_{z_j} n_e S_{z_j} + n_{z_{j-1}} n_e S_{z_{j-1}} + n_{z_{j+1}} n_e \alpha_{z_{j+1}} - n_{z_j} n_e \alpha_{z_j} \quad j = 0 \rightleftharpoons Z$$

where S and α are the ionization and recombination rate, while:

$$\Gamma_z = -D \frac{fn_z}{fr} - Vn_z$$

These are a set of Z coupled differential equations



Impurity transport

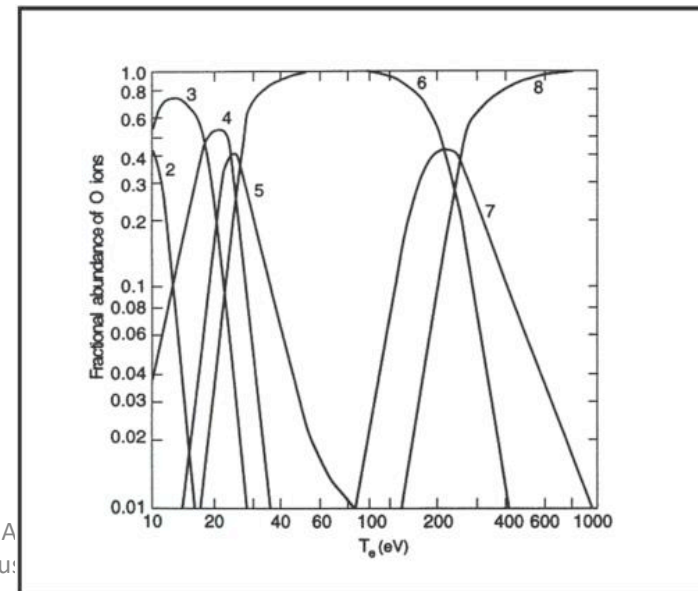
Solving this equations for all states is usually very complex, so that a series of assumptions are made:

Steady state $\left(d/dt = \partial/\partial t + \nabla \cdot = 0 \right)$

Neglect higher ionization state (Coronal equilibrium)

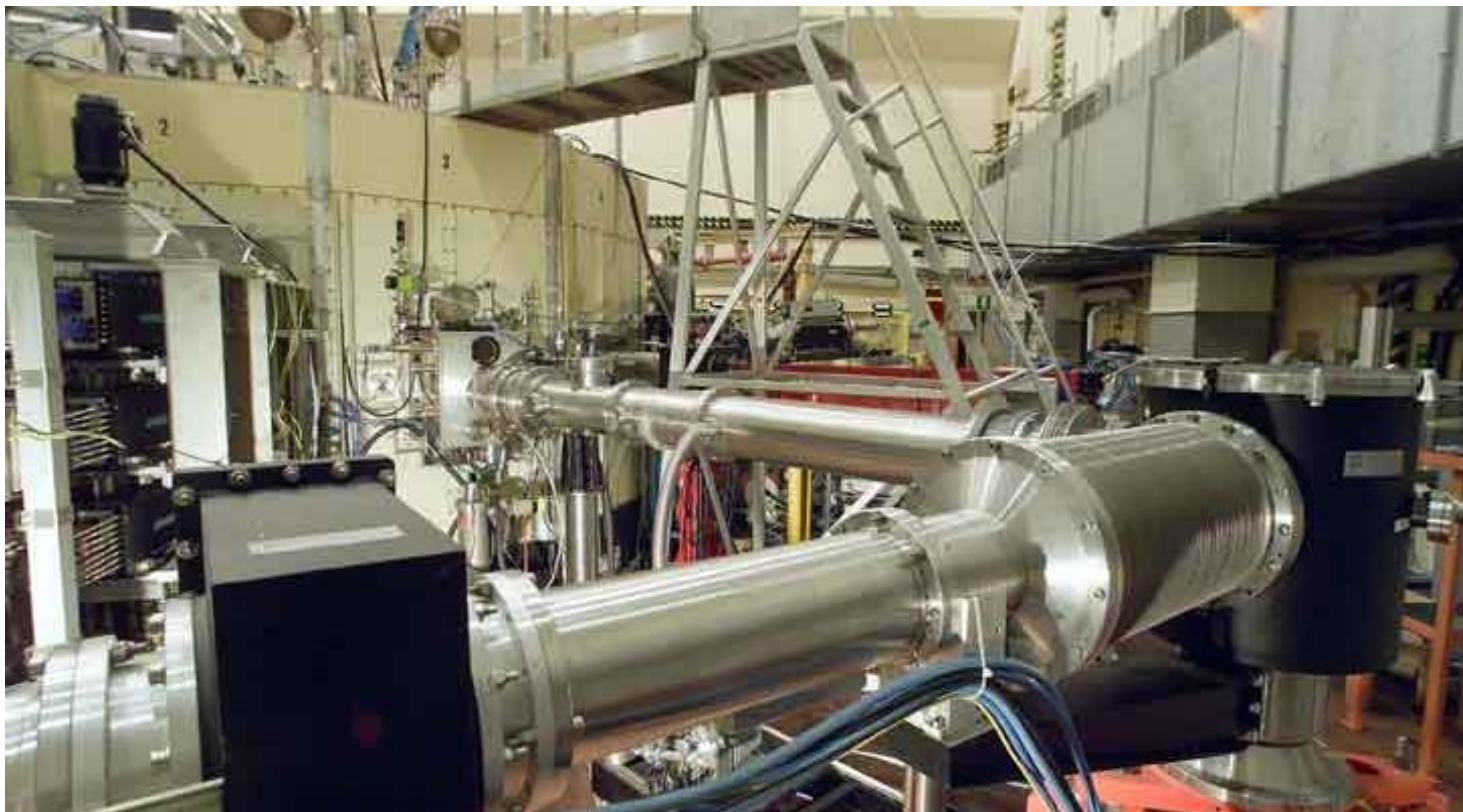
$$0 = n_{Z_{j-1}} n_e S_{Z_{j-1}} - n_{Z_j} n_e \alpha_{Z_j}$$

$$\frac{n_{Z_{j-1}}}{n_{Z_j}} = \frac{\alpha_{Z_j}}{S_{Z_{j-1}}}$$



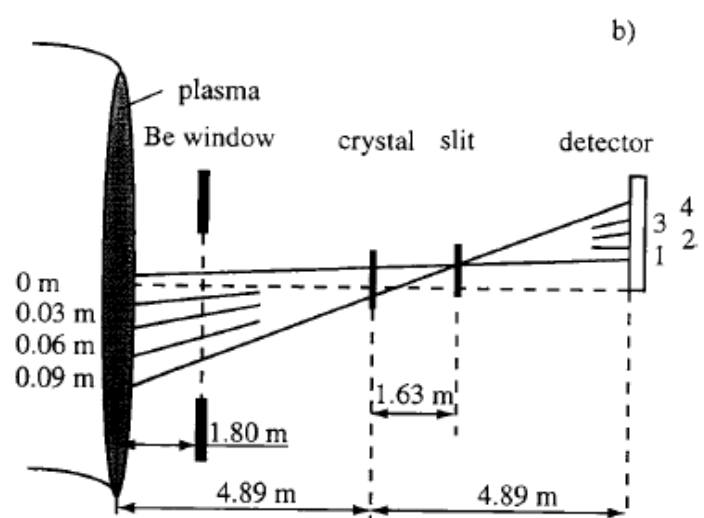
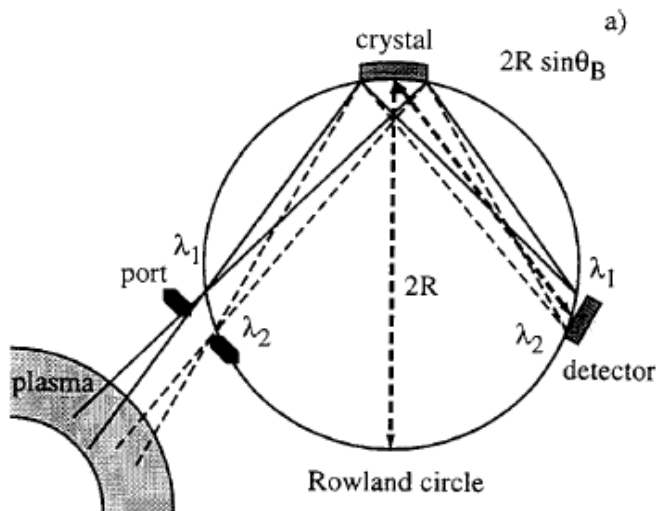
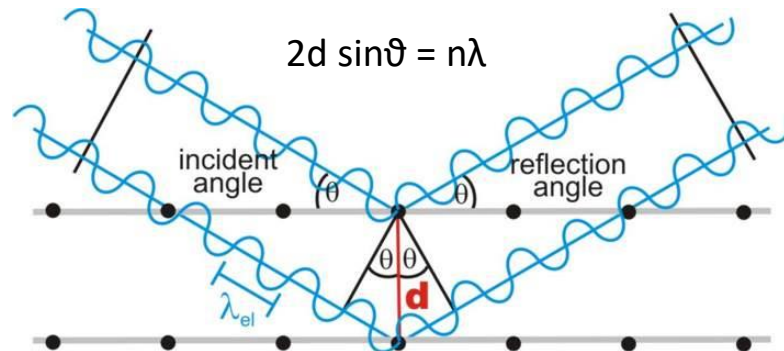
X-Ray spectrometer

FTU SXR high resolution spectrometer (not installed anymore)



X-Ray bent crystal

Bragg diffraction



X-Ray spectroscopy

SXR high resolution spectrum in Alcator C. Spectrum fitted with $T=1.2$ keV broadening.

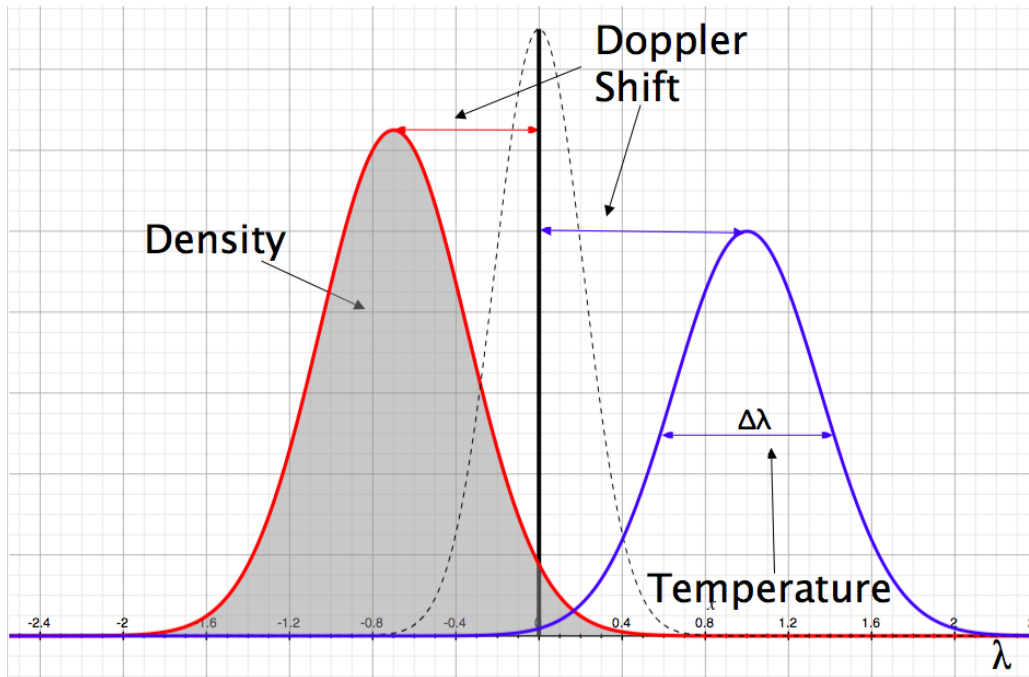
ity of 3.7 \AA ($= 0.37 \text{ nm}$) wavelength, a
e lines are visible: two are from the L
argon A^{17+} and a third is from moly
ominantly excited in the center of this
ybdenum line is noticeably narrower
e slowly owing to its greater mass. T
n the line widths are consistent (~ 1200
ertainty.

nother possibility for Doppler broad
emperature plasmas is to use certain “f

Information from spectral line

From line emission we can get :

- Density of impurity (area below the line)
- Temperature (line width)
- Average velocity along the line sight (Doppler Shift)



Rotation from Doppler shift

Plasma rotation speed from High resolution SXR spectroscopy on PLT during NBI injection

Fig. 6.16. Measurements of plasma flow velocity using different impurity species. The injection of energy causes this tokamak plasma to rotate toroidally. Prior to injection, the plasma was stationary. The rotation speed was measured by Doppler shift of the impurity lines [after Suckewer *et al.* (1979)].

Generally speaking, the presence of thermal broadening will set a lower limit to the detectable line shift. However, if the thermal Doppler width, the fraction depending on the temperature of the broadened line can be determined, the rotation speed levels (see Exercise 6.13).

Because the thermal velocity is inversely proportional to the square root of the mass of the species, heavier ions will generate a larger shift of line width to line shift (assuming their mean